CHAPTER 3

Synthesis and characterization of mixed ligand Ruthenium(II)-polypyridyl complexes.

Four different series of ruthenium (II) phenanthroline compounds of the general structural formula [Ru(*phen*)$_2$(*L*)]ClO$_4$ (*phen* = 1,10-phenanthroline; *L* = N, O and O, O donor ligands discussed in previous chapter i.e. Inh 1-4, FcA 1-4, Isa 1-4, Flq 1-3) have been synthesized and characterized by means of ESI mass spectrometry, FTIR and UV-Vis spectroscopy. The complexes so formed were found to be octahedral in geometry with all the six coordination sites taken up by non dissociable ligands resulting into chemically stable complexes.

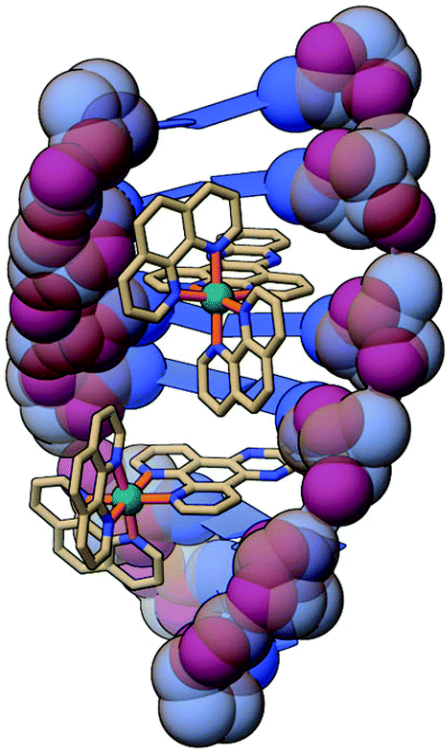

Section 3.4 of this chapter is based on the article: Pulipaka Ramadevi, Rinky Singh, Sarmita S Jana, Ranjitsinh Devkar, Debjani Chakraborty* *Journal of Photochemistry and Photobiology A: Chemistry*, **2015**, *305*, 1-10.

TABLE OF CONTENTS

3.1 Introduction to Ruthenium(II)-polypyridyl complexes:

3.1.1 Importance of Ru(II) polypyridyl complexes focusing on *1,10-phenanthroline*:

Polypyridyl metal complexes have remained one of the most important areas of research in transition metal based biological inorganic chemistry, specifically in their application as DNA binding agents, as cytotoxic and antibacterial agents, and as enzyme inhibitors [1]. Metallo-intercalators, -insertors, and -groove binders have been of interest for many years, and are the subject of numerous recent reviews [2-4]. In 1952 the Australian chemist Francis Dwyer and co-workers published a landmark study outlining the biological activity of several polypyridyl transition metal complexes (*Fig.3.1*) [5,6]. These simple complexes displayed diverse biological activities, including toxicity in mice, inhibition of the enzyme acetylcholinesterase, and bacteriostatic/bacteriocidal action against *Escherichia coli* and *Staphylococcus haemolyticus*.

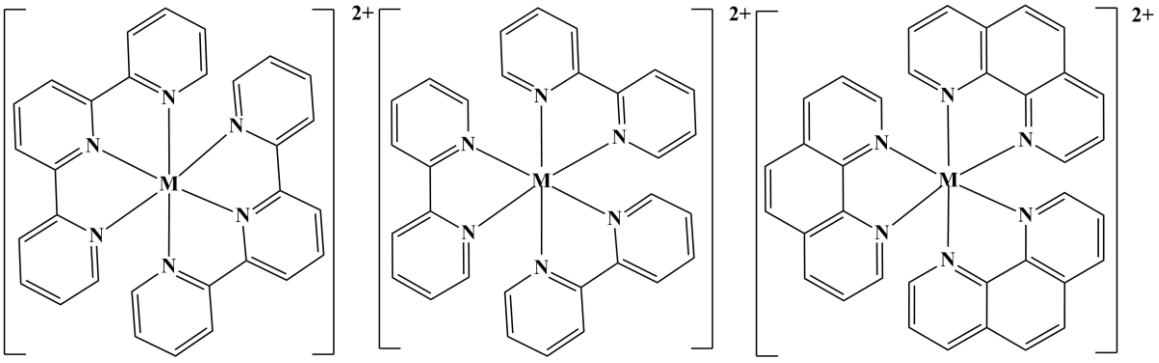

A [M(*tpy*)$_3$] **B** [M(*bpy*)$_3$] **C** [M(*phen*)$_3$]

Fig. 3.1: *Metal complexes tested for biological activity by Dwyer and co-workers in 1952 (**A** [M=Ru], **B** [M=Ru, Os], **C** [M=Fe, Ni, Ru, Os]). (tpy = 2,2':6'2''-terpyridine, bpy = 2,2'-bipyridine, phen = 1,10-phenanthroline)*

Dwyer's most significant work on biological inorganic chemistry was characterised by the application of archetypical tris-homoleptic ruthenium (II) polypyridyl complexes [7]. The work of Dwyer established the interactions of chemically, stereochemically, redox and configurationally stable ruthenium (II) polypyridyl complexes with an incredibly broad range of biological targets. The stability of ruthenium (II) polypyridyl complexes in biological systems is a key feature and allows for the development of specific toxicities and actions arising from the complex acting as a unit. As stated by Dwyer in 1959: '*When all of the coordination positions about a metal ion are taken up by non-dissociable ligands, no chemical bonds can be formed between the metal and protein. Any biological action must be purely physical.*'[8]. The metal in these systems serves two purposes:

- A structural role, by projecting the coordinated ligands into three-dimensional space and thereby determining the complex geometry and ability to fit into a given target; and
- As a source of positive charge, enabling the formation of attractive electrostatic interactions with biomolecular surfaces.

The choice of ligands also determines other pharmacological properties, since the binding of hydrophobic complexes to biomolecular surfaces is not only entropically favourable through dehydration processes, but the higher complex cation lipophilicity also increases the penetration of the complexes through biological membranes. Simple tris-1,10-phenanthroline complexes, such as $[Ru(phen)_3]^{2+}$ (*Fig. 3.1 C*), bind to both the DNA minor groove (L enantiomer) and as partial intercalators (D enatiomer) [9]. Further expansion of the intercalating ligand scaffold, increasing the central charge on the metal and modifying the remaining coordination sphere has provided complexes capable of sequence recognition. These DNA binding metal complexes are increasingly applied as structural probes and for in vivo studies of cytotoxicity [1]. Polypyridyl metal complexes, such as **D** and **E** (*Fig. 3.2*), have been demonstrated to be as cytotoxic as the well known anticancer agent cisplatin against several carcinogenic cell lines [10,11].

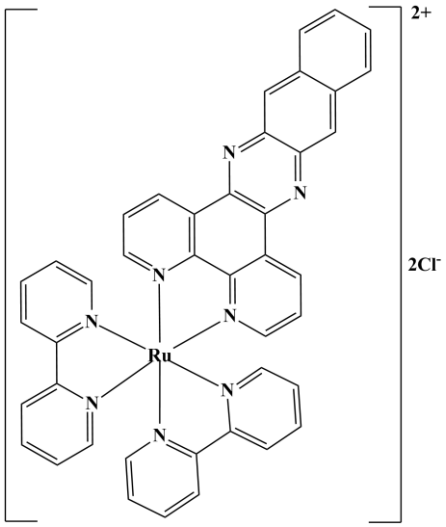

D

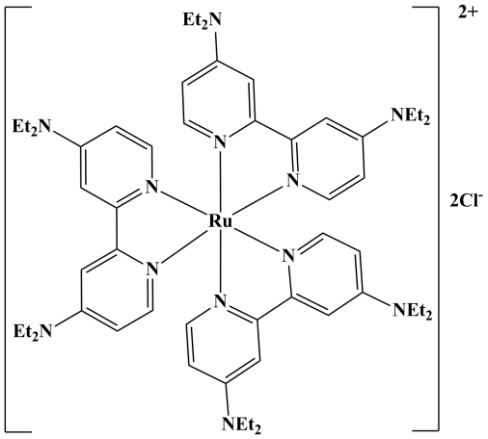

E

Fig. 3.2: *Cytotoxic complexes **D** and **E***

Few more examples of these compounds are $[Ru(tpy)Cl_3]$ and α-$[Ru(azpy)_2Cl_2]$ (*azpy = 2-phenylazopyridine*). $Ru(tpy)Cl_3$ shows a pronounced *in vitro* cytotoxicity and exhibits antitumor activity [12]. The compound α-$[Ru(azpy)_2Cl_2]$ has been reported to show a remarkably high cytotoxicity, even more pronounced than cisplatin in most of the tested cell lines [13,14]. The increased number of possible binding modes of ruthenium

polypyridyl complexes to DNA as compared to those of the first generations of platinum drugs and intercalation of the ligands between two parallel base pairs, could be crucial in order to overcome resistance to cisplatin [15].

❖ **Phenanthroline ligand *versus* other polypyridyl ligands:**

Although polypyridyl ruthenium (II) complexes are resistant to susbstitution and therefore unlikely to covalently bond with biomolecules, they are capable of either photosensitizing or intercalating into DNA. Additional uses for this class of compounds abound are such as their use as cellular imaging agents [16] and catalysts [17]. The ability of Ru(II) polypyridyl complexes to bind DNA relies closely on the ligands chosen for the complex. For example, a comparitive study between [Ru(*Clazpy*)$_2$(*bpy*)]Cl$_2$.7H$_2$O and [Ru(*Clazpy*)$_2$(*phen*)]Cl$_2$.8H$_2$O (*Clazpy = 5-chloro-2-(phenylazo)-pyridine*) showed the latter to have better cleavage and intercalation abilities due to the increased hydrophobicity, π-stacking ability, planarity, and lack of steric hindrance of the phenyl group when compared to the *bpy* ligand [18]. Another comparative study on pBR322 binding of [Ru(*phen*)$_2$(*DMDPPZ*)](ClO$_4$)$_2$ and [Ru(*dmp*)$_2$(*DMDPPZ*)](ClO$_4$)$_2$ (*DMDPPZ = 3,6-dimethyldipyrido[3,2-a:2',3'-c]phenazine, dmp = 2,5-dimethylpyrrole*) (*Fig. 3.3*) also found the less bulky first compound to be more efficient at single stranded DNA cleavage because of better intercalation, due to the absence of methyl groups on the phenyl ligands [19].

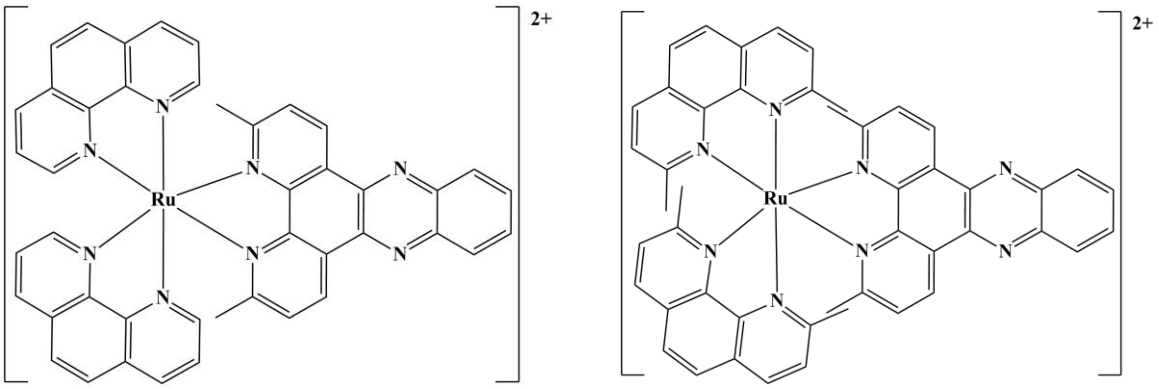

F **G**

Fig. 3.3: *Structures of complexes **F** - [Ru(phen)$_2$(DMDPPZ)](ClO$_4$)$_2$ and **G** - [Ru(dmp)$_2$(DMDPPZ)](ClO$_4$)$_2$*

However, simple metal complexes, such as [Ru(*bpy*)$_3$]$^{2+}$, that interact with DNA solely through electrostatic effects usually possess very low binding affinities. The archetypical ruthenium-based metallo-intercalators are the much studied

$[Ru(bpy)_2(dppz)]^{2+}$ and $[Ru(phen)_2(dppz)]^{2+}$ cations (*dppz = dipyridophenazine*). In 1990, the Barton and Sauvage groups reported that these *phen* and *dppz*-based complexes bind to DNA with a high affinity (equilibrium binding constant, $K_b \sim 10^6 M^{-1}$) and, interestingly, *dppz*-based complexes display intense MLCT-based (MLCT = metal-to-ligand charge-transfer) luminescence on the addition of DNA [20,21].

3.1.2 Past, Present and Future perspectives of Ru(II) polypyridyl complexes:

From a synthetic perspective, one of the most attractive aspects of metal polypyridyl chemistry is the flexibility of synthesis, as it is possible to generate several closely-related molecules that may be investigated in structure–activity studies. The biological mode of action of these complexes is mediated through their ligand sphere, as demonstrated by the distinct biological properties of configurationally stable stereoisomers. Today, more than half a century later, building on the pioneering contributions of Dwyer and co-workers, the octahedral coordination geometry of ruthenium polypyridyl complexes permits the construction of sophisticated globular and often rigid structures whose rich stereochemistry and chelation induced conformational restrictions can be successfully exploited for the design of inert and selective metal-based nucleic acid binders and enzyme inhibitors. It should be pointed out that in future studies DNA may not be the only biomolecular structure targeted by reversible binding of metal polypyridyl complexes: in a recent study Olga *et al* examined the photophysical properties of ruthenium(II) complexes comprising two 4,7-diphenyl-1,10-phenanthroline (dip) ligands and functionalized bipyridine (R_1bpy-R_2, where R_1 = H or CH_3, R_2 = H, CH_3, COO-,4-[3-(2-nitro-1H-imidazol-1-yl)propyl] or 1,3-dicyclohexyl-1-carbonyl-urea) towards development of luminescence probes for cellular imaging. These complexes have been shown to interact with albumin and the formed adducts exhibited up to eightfold increase in the luminescence quantum yield as well as the average lifetime of emission [22]. In another such study Marija *et al* qualitatively and quantitatively determined ruthenium binding sites on a protein. The binding of two Ru(II) complexes of a meridional geometry, namely mer-$[Ru(4'Cl\text{-}tpy)(en)Cl]^+$ and mer-$[Ru(4'Cl\text{-}tpy)(dach)Cl]^+$ (where 4′ Cl-tpy = 4′-chloro-2,2′:6′,2″-terpyridine, en = 1,2-diaminoethane and dach = 1,2-diaminocyclohexane), to bovine serum albumin was investigated by means of size exclusion- and reversed phase-LC (liquid chromatography), ICP OES (inductively coupled plasma optical emission spectrometry), matrix-assisted laser desorption ionization MS and MS/MS. Ruthenated peptide sequence and a binding target amino acid were revealed through accurate elucidation of MS/MS spectra. The results obtained in this study suggest a high binding capacity of the protein towards both complexes, with up

to 5.77 ± 0.14 and 6.95 ± 0.43 mol bound per mol of protein. The proposed binding mechanism for the selected complexes includes the release of Cl^- ligand, its replacement with water molecule and further coordination to electron donor histidine residue [23].

It seems to be only a question of time until such complexes will be developed into clinically used therapeutic and diagnostic agents.

In line with the above mentioned facts and review of development of ruthenium polypyridyl complexes as potent anticancer agents, four different series of ruthenium (II) phenanthroline compounds of the general structural formula $[Ru(phen)_2(L)]ClO_4$ (*phen* = 1,10-phenanthroline; *L* = N, O and O, O donor ligands) have been synthesized and characterized using various spectroscopic methods with an aim to be further investigated upon for their biological activities.

3.2 General synthesis of [Ru(phen)$_2$ L]ClO$_4$ complexes:

3.2.1 Materials and instrumentation:

All the chemicals and solvents used for the synthesis and characterization of [**Ru(*phen*)$_2$L**]**ClO$_4$** complexes are of analytical grade and were used as purchased. The precursor [Ru(*phen*)$_2$Cl$_2$] was prepared according to the procedure sited in literature [24]. 1,10-phenathroline was purchased from Qualigens. $RuCl_3$. $3H_2O$ was purchased from Hi-media (Mumbai, India) and sodium perchlorate was purchased from Acros organics (United States).

ESI Mass spectra of the complexes were recorded on Applied Biosystem API 2000 Mass spectrometer. Infrared spectra (400-4000cm^{-1}) were recorded on Perkin Elmer RX-1 FTIR with samples prepared as KBr pellets. UV–visible spectra were recorded in 1:1 DMSO:H_2O solutions at concentrations around 10^{-3} M on Perkin Elmer Lambda-35 dual beam UV-Vis spectrophotometer. C, H and N elements of the complexes were estimated using Thermo Scientific Flash 2000 elemental analyzer. The molar conductance of the complexes was measured in DMSO at 10^{-3} M concentration using Toshniwal conductivity bridge Type CLOI/O1A with a dip type conductivity cell.

3.2.2 General synthetic scheme:

A mixture of the precursor [Ru(*phen*)$_2$Cl$_2$] $2H_2O$ and the synthesized ligand (**L**) (*Ch 2*) in 1:1 mole ratio was refluxed in 3 ml of ethanol: water (2:1) mixture for 7 hours to form a clear red solution. Upon cooling saturated aqueous solution of sodium perchlorate ($NaClO_4$) was added drop wise and stirred for 2 hours at r.t. The reaction mixture was sealed under nitrogen and cooled at 0°C for overnight. On addition of water, immediate reddish brown precipitates were obtained which were filtered, washed with water and dried in oven at 50°C for 3 hours. The product so obtained was recrystallized from hot methanolic solution resulting in reddish brown crytstalline product but not of single crystal quality. *Fig. 3.4* shows the general synthetic route of [**Ru(*phen*)$_2$L**]**ClO$_4$** complexes.

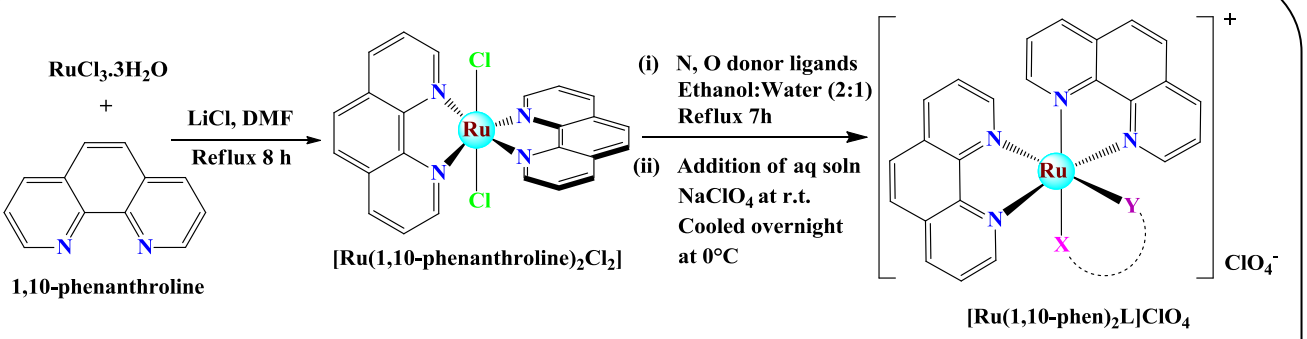

Fig. 3.4: *General synthetic scheme of [**Ru(phen)$_2$L]ClO$_4$** complexes.*

Where, **L** stands for the synthesized ligands (discussed in *Ch.2*)

Table 3.1: *List of the different ligand series used in the synthesis of [Ru(Phen)$_2$L]ClO$_4$ complexes along with their coordinating sites to the Ru(II) centre.*

L = Ligands	*Ligand codes*	*Complex codes*	*X*	*Y*
Isoniazid derivatives	**Inh 1-4**	**RPInh 1-4**	N	O
Ferrocenyl derivatives	**FcA 1-4**	**RPFcA 1-4**	N	O
Isatin derivatives	**Isa 1-4**	**RPIsa 1-4**	N	O*
Fluoroquinolones	**Flq 1-3**	**RPFlq 1-3**	O	O

***Note:** in case of **RPIsa-4** Y=S*

The composition and structures of all the **[Ru(*Phen*)$_2$L]ClO$_4$** complexes have been confirmed by ESI Mass spectrometry, FTIR, UV-Vis spectroscopy, elemental analysis and conductance measurements. The analytical data are consistent with the proposed structures and their empirical formulas.

3.3 [Ru(phen)$_2$ (Inh 1-4)]ClO$_4$ complexes: (RPInh 1-4)

3.3.1 Synthesis and characterization:

[Ru(phen)$_2$(Inh-1)]ClO$_4$ **(RPInh-1):**

[Ru(*phen*)$_2$Cl$_2$] 2H$_2$O (0.0528 mmol, 30.0 mg) and **Inh-1** (0.0528 mmol, 11.9 mg) was used to synthesize **RPInh-1**. Solubility: DMSO, DMF. Complete solubility was also achieved in DMSO-H$_2$O in the ratio 1:2. Yield: 85.3%; Molecular Weight 785.17 g/mol; Molecular Formula $C_{37}H_{26}ClN_7O_5Ru$; Anal. Found: C, 55.01; H, 3.34; N, 10.98. Calc.: C, 56.60; H, 3.34; N, 12.49. ESI-MS *m/z*: 686 (M^+ - ClO_4^-), 496 $[Ru(phen)_2NH_2OH]^+$, 325 $[Ru(Inh\text{-}1)]^+$, 99 (ClO_4^-); FTIR (KBr, ν/cm^{-1}): $\nu_{C=N}$ 1670, ν_{C-O} 1070, ν_{Cl-O} 628.

[Ru(phen)$_2$(Inh-2)]ClO$_4$ **(RPInh-2):**

[Ru(*phen*)$_2$Cl$_2$] 2H$_2$O (0.0528 mmol, 30.0 mg) and **Inh-2** (0.0528 mmol, 12.7 mg) was used to synthesize **RPInh-2**. Solubility: DMSO, DMF. Complete solubility was also achieved in DMSO-H$_2$O in the ratio 1:2. Yield: 88.09%; Molecular Weight 801.17 g/mol; Molecular Formula $C_{37}H_{26}ClN_7O_6Ru$; Anal. Found: C, 53.59; H, 3.04; N, 11.98. Calc.: C, 55.47; H, 3.27; N, 12.24. ESI-MS *m/z*: 700.3 (M^+-2-ClO_4^-), 494 $[Ru(phen)_2NH_2OH]^+$, 341 $[Ru(Inh\text{-}2)]^+$, 98.9 (ClO_4^-); FTIR (KBr, ν/cm^{-1}): $\nu_{C=N}$ 1681, ν_{C-O} 1085, ν_{Cl-O} 624.

[Ru(phen)$_2$(Inh-3)]ClO$_4$ **(RPInh-3):**

[Ru(*phen*)$_2$Cl$_2$] 2H$_2$O (0.0528 mmol, 30.0 mg) and **Inh-3** (0.0528 mmol, 14.3 mg) was used to synthesize **RPInh-3**. Solubility: DMSO, DMF. Complete solubility was also achieved in DMSO-H$_2$O in the ratio 1:2. Yield: 81.8%; Molecular Weight 831.19 g/mol; Molecular Formula $C_{38}H_{28}ClN_7O_7Ru$; Anal. Found: C, 52.93; H, 3.52; N, 10.67. Calc.: C, 54.91; H, 3.40; N, 11.80. ESI-MS *m/z*: 732.4 (M^+-ClO_4^-), 495.3 $[Ru(phen)_2NH_2OH]^+$, 98.9 (ClO_4^-); FTIR (KBr, ν/cm^{-1}): $\nu_{C=N}$ 1665, ν_{C-O} 1079, ν_{Cl-O} 626.

[Ru(phen)$_2$(Inh-4)]ClO$_4$ **(RPInh-4):**

[Ru(*phen*)$_2$Cl$_2$] 2H$_2$O (0.0528 mmol, 30.0 mg) and **Inh-4** (0.0528 mmol, 13.4 mg) was used to synthesize **RPInh-4**. Solubility: DMSO, DMF. Complete solubility was also achieved in DMSO-H$_2$O in the ratio 1:2. Yield: 88.3%; Molecular Weight 815.19 g/mol; Molecular Formula $C_{38}H_{28}ClN_7O_6Ru$; Anal. Found: C, 53.36; H, 2.99; N, 11.85. Calc.: C, 55.99; H, 3.46; N, 12.03. ESI-MS *m/z*: 718 (M^++2-ClO_4^-), 494.2 $[Ru(phen)_2NH_2OH]^+$, 99 (ClO_4^-); FTIR (KBr, ν/cm^{-1}): $\nu_{C=N}$ 1668, ν_{C-O} 1087, ν_{Cl-O} 625.

3.3.2 Results and discussion:

The IR spectra of **RPInh 1-4** lack the strong secondary amide carbonyl absorption at 1670-1700 cm^{-1} that is typically seen in the spectra of the free ligands **Inh 1-4**. Coordination of the Schiff bases to the metal through the nitrogen atom is expected to reduce the electron density in the azomethine frequency. In all the four complexes, the band due to azomethine nitrogen $\nu_{C=N}$ shows a modest decrease in the stretching frequency and is shifted to lower frequencies, appearing around 1570-1610 cm^{-1}, which indicates the coordination of the azomethine nitrogen to the metal [25]. Moreover the enolate structure of the coordinated ligand is supported by a band at 1059-1060 cm^{-1} due to the enolic C-O stretching [26]. The N-H stretching band between 3150-3250 cm^{-1} found in the IR spectra of ligands (*Sec. 2.2.4*) are completely lost in the spectra of their complexes **RPInh 1-4** which is also indicative of the enolization and deprotonation on coordination. The presence of perchlorate as the counter ion in the complexes is indicated by its ν_{Cl-O} stretching band in the range of 625-635 cm^{-1} [27].

The electronic absorption spectra of the complexes show three major bands in the wavelength range 200-900 nm. In the UV-Vis spectra of **RPInh 1-4** (*Fig.3.5*)**,** the first band appearing at around 226-227 nm can be assigned to the $\pi \rightarrow \pi^*$ transition of the aromatic rings. The second band observed within 264-268 nm can be assigned to the azomethine based intra-ligand $n \rightarrow \pi^*$ transition [28] slightly shifted to shorter wavelength on going from ligand to complex, indicating coordination of ligand to metal through the azomethine moiety [29]. A broad and distinct band appears in the range of 390-420 nm for all the four complexes attributable to $d\pi \rightarrow \pi^*$ MLCT (metal to ligand charge transfer) transitions [30]. Also all the four complexes show ruthenium(II) centered d-d transition bands in the region 670-680 nm. The λ_{max} values of all the transitions taking place in **RPInh 1-4** have been tabulated in *Table 3.2*.

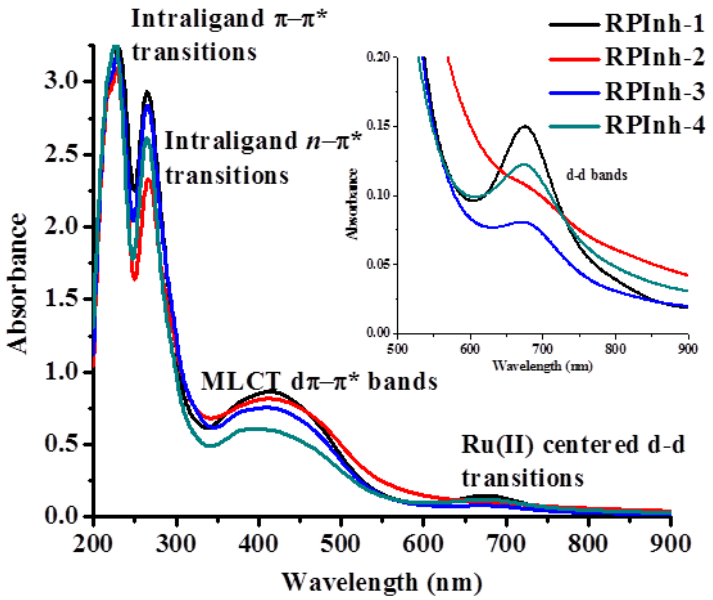

Fig. 3.5: *UV-vis. spectra of complexes* ***RPInh 1-4*** *recorded in DMSO with path length 1 cm. (Inset: Expanded spectra of* ***RPInh 1-4*** *indicating the ruthenium(II) centered d-d bands)*

Table 3.2: *UV-Vis peak assignments and conductance measurements of* ***RPInh 1-4***

Compound	*Intra-ligand Transitions (nm)*		*MLCT dπ-π* transitions (nm)*	*d-d transitions (nm)*	Λ_m *($\Omega^{-1}cm^2mole^{-1}$)*
	*π-π**	*n-π**			
RPInh-1	227	264	416	676	34.7
RPInh-2	227	267	417	678	22.7
RPInh-3	226	268	414	674	25.2
RPInh-4	227	267	392	675	25.7

All the four complexes **RPInh 1-4** have molar conductances (1x 10^{-3}M in DMSO) in the range of 22 - 35 $\Omega^{-1}cm^2mole^{-1}$ (*Table 3.2*) suggesting 1:1 electrolytic behavior. [31,32]

The ESI-MS positive ion spectra of **RPInh 1-4** given in *Fig. 3.6* show peaks corresponding to *m/z* = 686.1 (M^+-ClO_4^-) **RPInh-1**, 700.3 (M^+-2-ClO_4^-) **RPInh-2**, 732.4 (M^+-ClO_4^-) **RPInh-3** and 718.3 (M^++2-ClO_4^-) **RPInh-4**. All the peaks have been tabulated in *Table 3.3* showing the main fragments obtained. The negative ion spectra (*Fig. 3.7*) of all the four complexes show a prominent peak at *m/z* = 99 attributed to the perchlorate ion present as the counter anion. The *m/z* values indicate that two 1,10-phenanthroline ligands (N,N donor) and one Schiff base ligand (N,O donor) are coordinated to the metal centre in the complexes.

Table 3.3: *m/z values of complexes* ***RPInh 1-4****showing fragmentation.*

Compound	*m/z values*	*Fragments*
RPInh-1	686	$[Ru(phen)_2(Inh\text{-}1)]^+$ ($M^+ - ClO_4^-$)
	496	$[Ru(phen)_2NH_2OH]^+$+1
	325	$[Ru(Inh\text{-}1)]^+$
	99	ClO_4^-
RPInh-2	700.3	$[Ru(phen)_2(Inh\text{-}2)\text{-}2]^+$ (M^+-2-ClO_4^-)
	494	$[Ru(phen)_2NH_2OH]^+$-1
	341	$[Ru(Inh\text{-}2)]^+$
	98.9	ClO_4^-
RPInh-3	732.4	$[Ru(phen)_2(Inh\text{-}3)]^+$ ($M^+ - ClO_4^-$)
	495.3	$[Ru(phen)_2NH_2OH]^+$
	98.9	ClO_4^-
RPInh-4	718	$[Ru(phen)_2(Inh\text{-}4)+2]^+$ (M^++2-ClO_4^-)
	494.2	$[Ru(phen)_2NH_2OH]^+$-1
	99	ClO_4^-

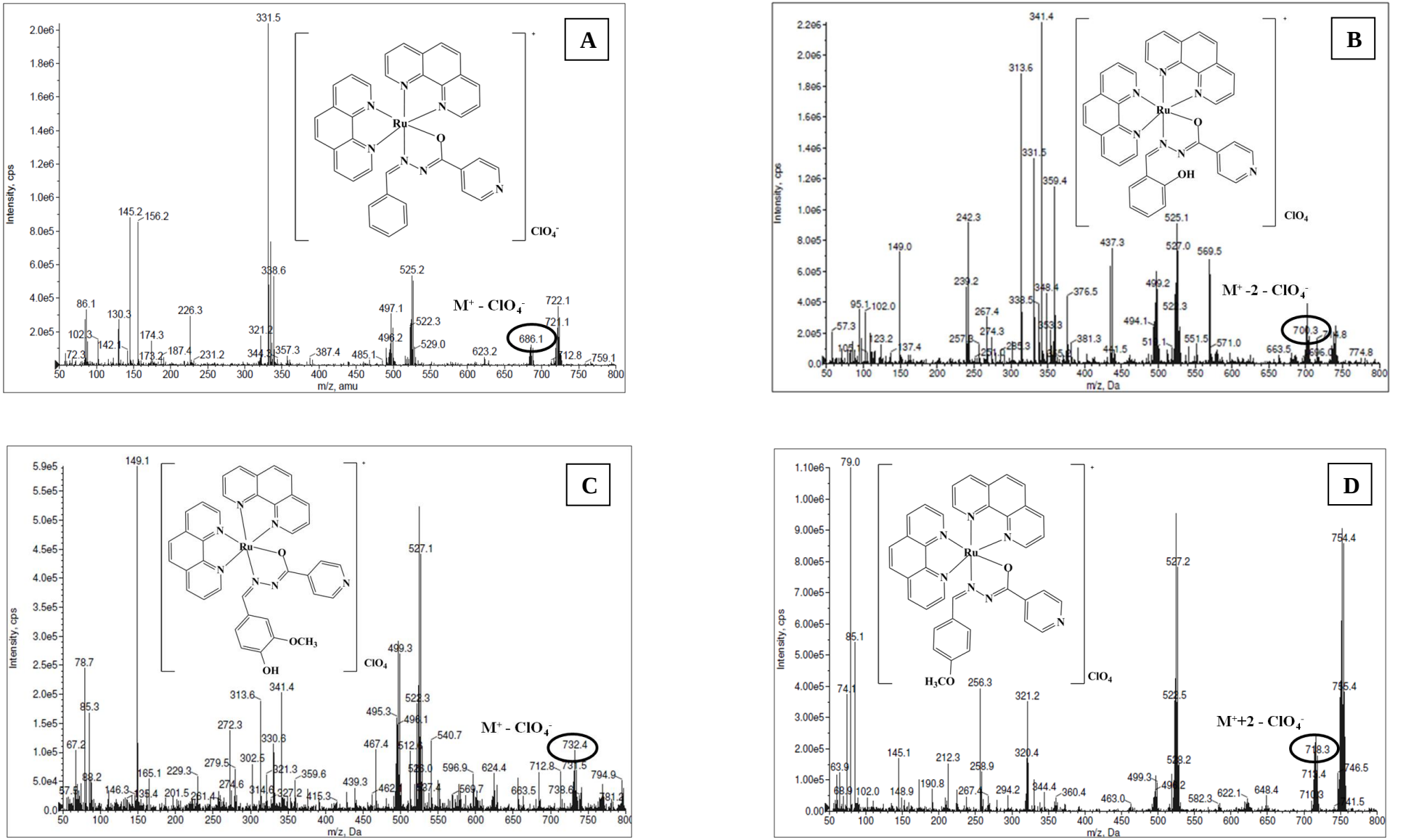

Fig. 3.6: *ESI-MS positive ion spectra of complexes (A)* ***RPInh-1*** *(B)* ***RPInh-2*** *(C)* ***RPInh-3*** *(D)* ***RPInh-4*** *indicating their molecular ion peak.*

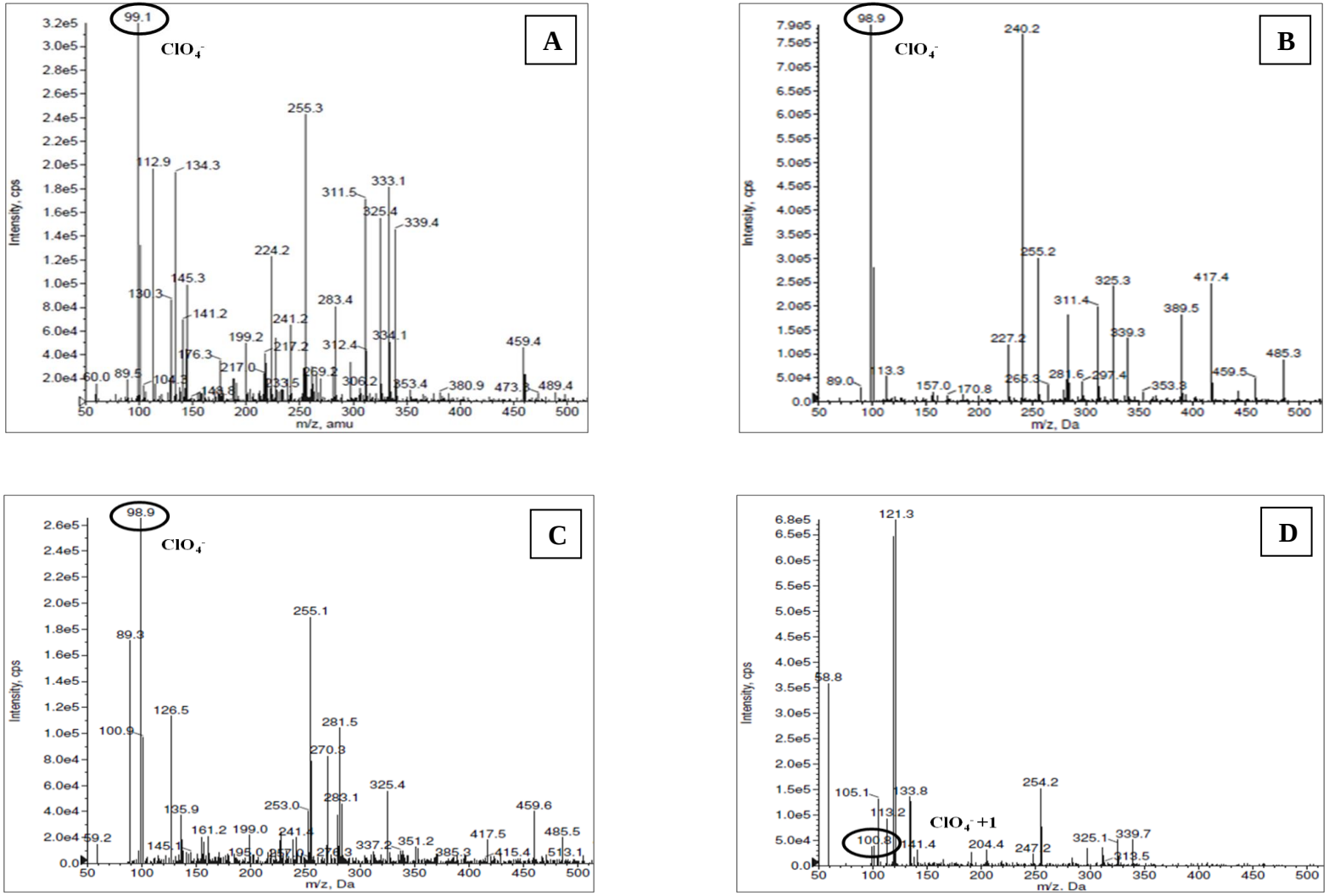

Fig. 3.7: *ESI-MS negative ion spectra of complexes (A)* ***RPInh-1*** *(B)* ***RPInh-2*** *(C)* ***RPInh-3*** *(D)* ***RPInh-4*** *indicating perchlorate ion peak.*

3.4 [Ru(phen)$_2$ (FcA 1-4)]ClO$_4$ complexes: (RPFcA 1-4)

3.4.1 Synthesis and characterization:

[Ru(phen)$_2$(FcA-1)]ClO$_4$ **(RPFcA-1):**

[Ru(*phen*)$_2$Cl$_2$] 2H$_2$O (0.0528 mmol, 30.0 mg) and **FcA-1** (0.0528 mmol, 20.0 mg) was used to synthesize **RPFcA-1**. Solubility: DMSO, DMF; Yield: 56.8%; Molecular Weight 939.17 g/mol; Molecular Formula $C_{44}H_{36}ClFeN_5O_7Ru$; Anal. Found: C, 56.5; H, 3.87; N, 7.61. Calc.: C, 56.27; H, 3.86; N, 7.46. ESI-MS *m/z*: 940.8 M^+; FTIR (KBr, ν/cm^{-1}): $\nu_{N\text{-}H}$ 3195, $\nu_{Cl\text{-}O}$ 627.

[Ru(phen)$_2$(FcA-2)]ClO$_4$ **(RPFcA-2):**

[Ru(*phen*)$_2$Cl$_2$] 2H$_2$O (0.0528 mmol, 30.0 mg) and **FcA-2** (0.0528 mmol, 19.2 mg) was used to synthesize **RPFcA-2**. Solubility: DMSO, DMF; Yield: 60.2%; Molecular Weight 923.15 g/mol; Molecular Formula $C_{44}H_{36}ClFeN_5O_6Ru$; Anal. Found: C, 57.81; H, 4.27; N, 7.73. Calc.: C, 57.25; H, 3.93; N, 7.59. ESI-MS *m/z*: 923.0 M^+; FTIR (KBr, ν/cm^{-1}): $\nu_{N\text{-}H}$ 3081, $\nu_{Cl\text{-}O}$ 624.

[Ru(phen)$_2$(FcA-3)]ClO$_4$ **(RPFcA-3):**

[Ru(*phen*)$_2$Cl$_2$] 2H$_2$O (0.0528 mmol, 30.0 mg) and **FcA-3** (0.0528 mmol, 17.4 mg) was used to synthesize **RPFcA-3**. Solubility: DMSO, DMF; Yield: 61.5%; Molecular Weight 889.14 g/mol; Molecular Formula $C_{41}H_{38}ClFeN_5O_6Ru$; Anal. Found: C, 55.32; H, 4.16; N, 7.84. Calc.: C, 55.38; H, 4.31; N, 7.88. ESI-MS *m/z*: 888.0 M^+; FTIR (KBr, ν/cm^{-1}): $\nu_{N\text{-}H}$ 3077, $\nu_{Cl\text{-}O}$ 625.

[Ru(phen)$_2$(FcA-4)]ClO$_4$ **(RPFcA-4):**

[Ru(*phen*)$_2$Cl$_2$] 2H$_2$O (0.0528 mmol, 30.0 mg) and **FcA-4** (0.0528 mmol, 21.2 mg) was used to synthesize **RPFcA-4**. Solubility: DMSO, DMF; Yield: 58.7%; Molecular Weight 962.19 g/mol; Molecular Formula $C_{46}H_{37}ClFeN_6O_6Ru$; Anal. Found: C, 57.58; H, 3.90; N, 8.76. Calc.: C, 57.42; H, 3.88; N, 8.73. ESI-MS *m/z*: 963.4 M^+; FTIR (KBr, ν/cm^{-1}): $\nu_{N\text{-}H}$ 3073, $\nu_{Cl\text{-}O}$ 625.

3.4.2 Results and discussion:

The FTIR spectra of the complexes **RPFcA 1-4** displayed characteristic strong stretching bands at 1520-1580 cm^{-1} and weaker bands at 1490-1514 cm^{-1} due to asymmetric and symmetric carboxylate (COO^-) stretch respectively which were found as strong bands in the fingerprint region at 1580-1610 cm^{-1} in the spectra of free **FcA 1-4**

ligands (*Sec. 2.3.4*). Moreover the distinct broad band at ~3450 cm^{-1} owing to the O-H stretching of free carboxylic acid group found in the ligand is completely lost in the IR spectra of the complexes indicating complexation of the ligand with metal via the carboxylate oxygen. Furthermore the medium secondary amine N-H stretching bands found in the spectra of the free ligands in the region 2900-3000 cm^{-1} was found to have a positive shift to 3080-3200 cm^{-1} in complexes indicating complexation of the ligand with metal via the nitrogen of secondary amine (mannich base). The presence of perchlorate as the counter ion in the complexes is indicated by its $\nu_{Cl\text{-}O}$ stretching band in the range of 625-635 cm^{-1} [27].

The electronic absorption spectra of the complexes **RPFcA 1-4** recorded in DMSO solution were in the region 200-900 nm. The electronic spectra of free ligands **FcA 1-4** displayed intense absorption bands at 207-209 nm and 270-300 nm ascribable to intra ligand $\pi \rightarrow \pi^*$ and $n \rightarrow \pi^*$ transitions respectively (*Fig. 2.8, Sec. 2.3.4*) which were observed to have shifted to longer wavelength region at 278-284 nm and 370-386 nm (*Fig. 3.8*) due to coordination with metal centre. The $n \rightarrow \pi^*$ transition bands are observed as low intensity peaks/shoulder in all the complexes. In addition all the complexes showed peaks in the region 460-500 nm corresponding to $d\pi \rightarrow \pi^*$ MLCT transitions. Furthermore, complexes showed ruthenium(II) centered distinct d-d bands in the visible region 690-710 nm. The absorption peak values have been tabulated in *Table 3.4*.

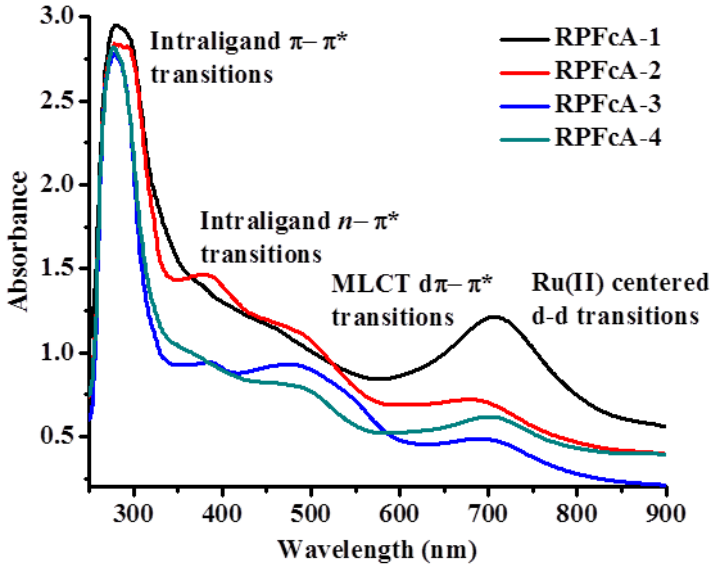

Fig. 3.8: *UV-Vis. spectra of complexes* ***RPFcA 1-4*** *recorded in DMSO with path length 1 cm.*

Table 3.4: *UV-Vis. peak assignments and conductance measurements of* ***RPFcA 1-4***

Compound	***Intra-ligand transitions (nm)***		***MLCT dπ-π* transitions (nm)***	***d-d transitions (nm)***	Λ_m ***($\Omega^{-1}cm^2mole^{-1}$)***
	π-π*	***n-π****			
RPFcA-1	280	380	464	709	36.7
RPFcA-2	284	386	492	695	32.5
RPFcA-3	278	385	488	707	34.2
RPFcA-4	279	370	496	705	37.2

All the four complexes **RPFcA 1-4** have molar conductances (1x 10^{-3}M in DMSO) in the range of 32 - 37 $\Omega^{-1}cm^2mole^{-1}$ (*Table 3.4*) suggesting 1:1 electrolytic behavior.

The ESI-MS spectra of the complexes showed molecular ion peaks with *m/z* values equivalent to their molecular weights. The *m/z* values of all the complexes are in well agreement with the proposed composition (*Fig. 3.9)* and have been tabulated in *Table 3.5*.

Table 3.5: *m/z values of complexes* ***RPFcA 1-4****showing fragmentation.*

Compound	***m/z values***	***Fragments***
RPFcA-1	940.8	$[Ru(phen)_2(FcA\text{-}1)]^+$ (M^+)
RPFcA-2	923.0	$[Ru(phen)_2(FcA\text{-}2)]^+$ (M^+)
RPFcA-3	888.0	$[Ru(phen)_2(FcA\text{-}3)]^+$ (M^+)
RPFcA-4	963.4	$[Ru(phen)_2(FcA\text{-}4)]^+$ (M^+)

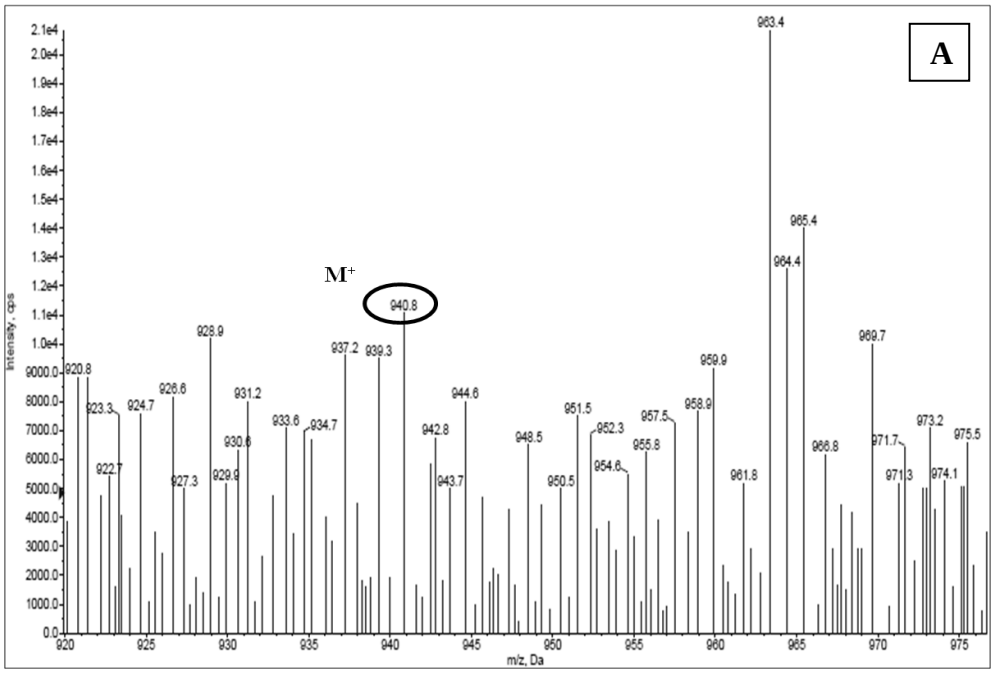
A
M+
940.8
963.4
965.4
964.4
969.7
928.9
937.2
939.3
931.2
926.6
944.6
959.9
958.9
957.5
951.5
952.3
955.8
948.5
954.6
950.5
961.8
966.8
971.7
973.2
975.5
920.8
923.3
924.7
922.7
927.3
929.9
930.6
933.6
934.7
942.8
943.7
971.3
974.1
Intensity, cps
m/z, Da

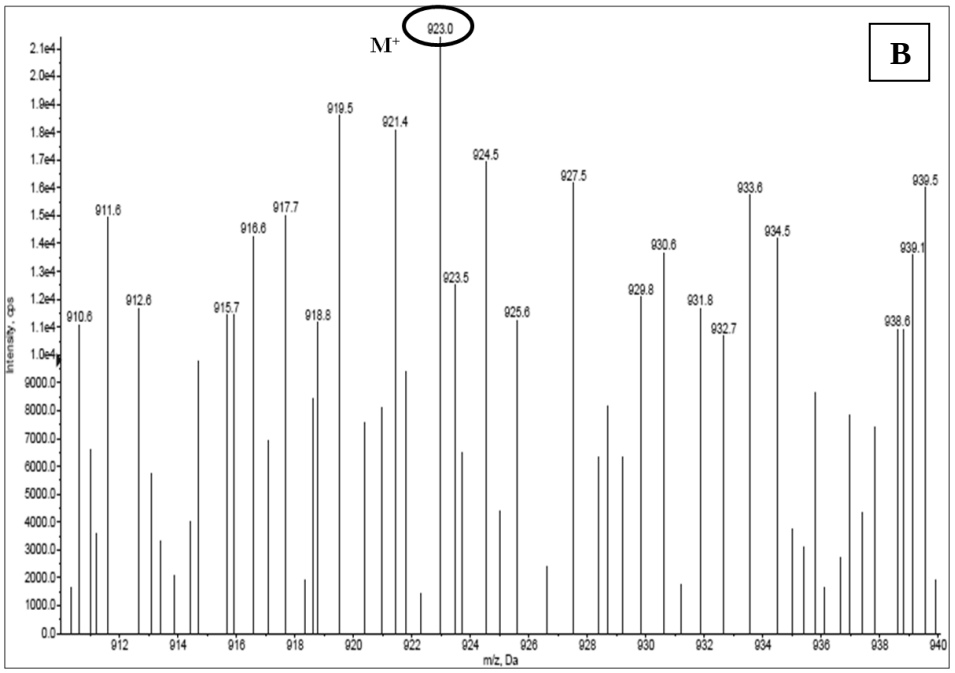
B
M+
923.0
919.5
921.4
924.5
927.5
933.6
939.5
911.6
916.6
917.7
930.6
934.5
939.1
910.6
912.6
915.7
918.8
923.5
925.6
929.8
931.8
932.7
938.6
Intensity, cps
m/z, Da

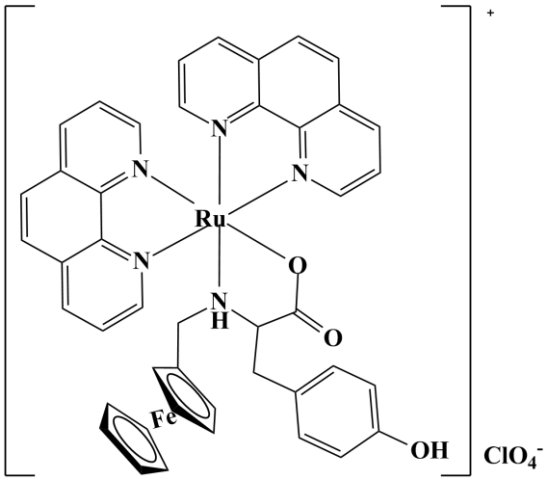
N
N
Ru
N
N
O
N
H
O
Fe
OH
ClO4-

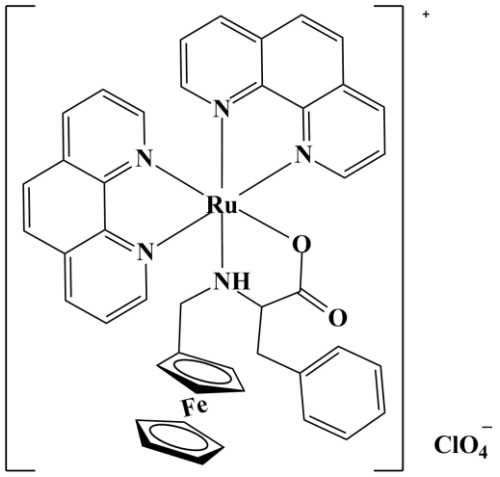
N
N
Ru
N
N
O
NH
O
Fe
ClO4−

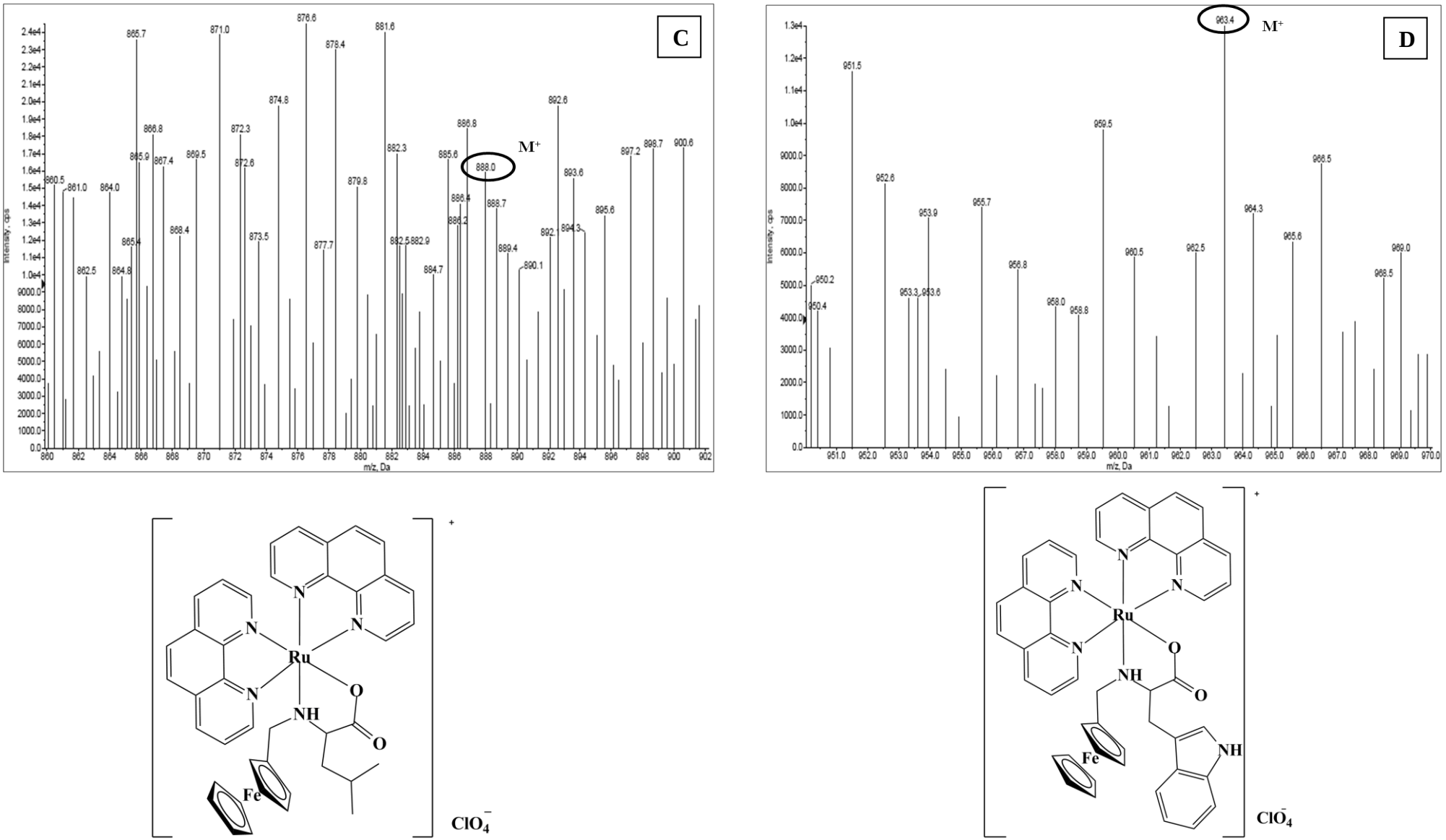

Fig. 3.9: *ESI-MS spectra of complexes (A)* ***RPFcA-1*** *(B)* ***RPFcA-2*** *(C)* ***RPFcA-3*** *(D)* ***RPFcA-4*** *indicating their molecular ion peak.*

3.5 [Ru(phen)$_2$ (Isa 1-4)]ClO$_4$ complexes: (RPIsa1-4)

3.5.1 Synthesis and characterization:

[Ru(phen)$_2$(Isa-1)]ClO$_4$ **(RPIsa-1):**

[Ru(*phen*)$_2$Cl$_2$] 2H$_2$O (0.0528 mmol, 30.0 mg) and **Isa-1** (0.0528 mmol, 14.0 mg) was used to synthesize **RPIsa-1**. Solubility: DMSO, DMF; Yield: 45.0%; Molecular Weight 825.19 g/mol; Molecular Formula $C_{39}H_{26}ClN_7O_6Ru$; Anal. Found: C, 54.53; H, 3.10; N, 10.69. Calc.: C, 56.76; H, 3.18; N, 11.88. ESI-MS *m/z*: 726.2 (M^+-ClO_4^-), 525.0 $[Ru(phen)_2OCH_2NHNH_2]^+$, 98.9 ($ClO_4^-$); FTIR (KBr/ cm^{-1}): $\nu_{(indolinic)N-H}$ 3051, $\nu_{(indolinic)C=O}$ 1670, $\nu_{C=N}$ 1541, ν_{C-O} 1093, ν_{Cl-O} 625.

[Ru(phen)$_2$(Isa-2)]ClO$_4$ **(RPIsa-2):**

[Ru(*phen*)$_2$Cl$_2$] 2H$_2$O (0.0528 mmol, 30.0 mg) and **Isa-2** (0.0528 mmol, 14.0 mg) was used to synthesize **RPIsa-2**. Solubility: DMSO, DMF; Yield: 51.3%; Molecular Weight 826.18 g/mol; Molecular Formula $C_{38}H_{25}ClN_8O_6Ru$; Anal. Found: C, 52.11; H, 3.00; N, 12.30. Calc.: C, 55.24; H, 3.05; N, 13.56. ESI-MS *m/z*: 726.1 (M^+-ClO_4^-), 525.0 $[Ru(phen)_2OCH_2NHNH_2]^+$, 98.9 ($ClO_4^-$); FTIR (KBr/ cm^{-1}): $\nu_{(indolinic)N-H}$ 3063, $\nu_{(indolinic)C=O}$ 1691, $\nu_{C=N}$ 1550, ν_{C-O} 1093, ν_{Cl-O} 620.

[Ru(phen)$_2$(Isa-3)]ClO$_4$ **(RPIsa-3):**

[Ru(*phen*)$_2$Cl$_2$] 2H$_2$O (0.0528 mmol, 30.0 mg) and **Isa-3** (0.0528 mmol, 10.7 mg) was used to synthesize **RPIsa-3**. Solubility: DMSO, DMF; Yield: 49.8%; Molecular Weight 764.11 g/mol; Molecular Formula $C_{33}H_{23}ClN_8O_6Ru$; Anal. Found: C, 49.66; H, 2.97; N, 12.94. Calc.: C, 51.87; H, 3.03; N, 14.66. ESI-MS *m/z*: 663.5 (M^+-2-ClO_4^-), 525.0 $[Ru(phen)_2OCH_2NHNH_2]^+$, 98.9 ($ClO_4^-$); FTIR (KBr/ cm^{-1}): $\nu_{(indolinic)N-H}$ 3061, $\nu_{(indolinic)C=O}$ 1691, $\nu_{C=N}$ 1565, ν_{C-O} 1091, ν_{Cl-O} 624.

[Ru(phen)$_2$(Isa-4)]ClO$_4$ **(RPIsa-4):**

[Ru(*phen*)$_2$Cl$_2$] 2H$_2$O (0.0528 mmol, 30.0 mg) and **Isa-4** (0.0528 mmol, 11.6 mg) was used to synthesize **RPIsa-4**. Solubility: DMSO, DMF; Yield: 55.1%; Molecular Weight 780.17 g/mol; Molecular Formula $C_{33}H_{23}ClN_8O_5SRu$; Anal. Found: C, 48.92; H, 2.95; N, 13.09. Calc.: C, 50.80; H, 2.97; N, 14.36. ESI-MS *m/z*: 681.2 (M^+-ClO_4^-), 525.0

$[Ru(phen)_2OCH_2NHNH_2]^+$, 98.9 ($ClO_4^-$); FTIR (KBr/ cm^{-1}): $\nu_{(indolinic)N-H}$ 3086, $\nu_{(indolinic)C=O}$ 1685, $\nu_{C=N}$ 1549, ν_{C-S} 848, ν_{Cl-O} 619.

3.5.2 Results and discussion:

The IR spectra of complexes **RPIsa 1-4** lack the strong secondary amide carbonyl absorption at 1680–1700 cm^{-1} that is typically seen in the spectra of the free ligands **Isa 1-4** (*sec. 2.5.4*). In all the complexes, $\nu_{C=N}$ band is shifted to lower frequency between 1540-1570 cm^{-1} indicating coordination of the Schiff bases through the azomethine nitrogen. The enolate structure of the coordinated ligand is supported by bands in the range of 1090-1093 cm^{-1} due to the enolic C-O stretching (C-S stretching at 848 cm^{-1} in case of **RPIsa-4**). The broad band found in the range of 3550-3600 cm^{-1} in the IR spectra of free ligands **Isa 1-4** due to the free amide N-H stretch are lost in the IR spectra of their complexes **RPIsa 1-4** which is also indicative of the enolization and deprotonation on coordination to the metal centre. The N-H stretching bands found in the range of 3050-3090 cm^{-1} are attributable to the indolinic N-H. Also in complexes **RPIsa 1-4** bands at 620-625 cm^{-1} are assignable to ν(Cl-O) stretch of the perchlorate ion.

The electronic absorption spectra of **RPIsa 1-4** (*Fig 3.10)* recorded in DMSO solution showed a sharp intense ligand based π→π* band at a wavelength range of 225-230 nm whereas the indolinic N, O centred intra ligand *n*→π* bands seen in the spectra of free ligands **Isa 1-4** between 270-275 nm (*Fig. 2.17, Sec. 2.5.4*) have blue shifted to ~265 nm while those found in the region 320-360 nm is found to have disappeared in the spectra of complexes **RPIsa-3** and **4** indicating coordination of the ligands to the metal centre through the hetero atoms. The complexes also showed peaks in the region 345-420 nm attributable to dπ→π* MLCT transitions as well as ruthenium(II) centered distinct d-d bands in the visible region 677-679 nm. The absorption peak values have been tabulated in *Table 3.6*.

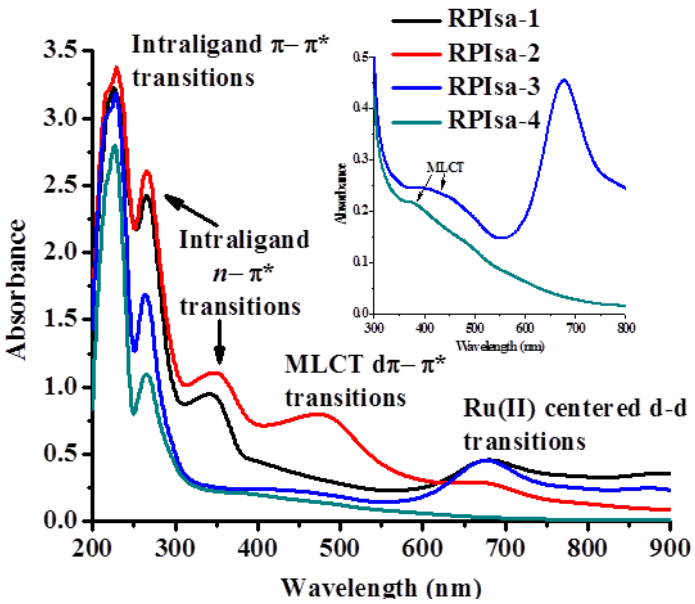

Fig. 3.10: *UV-Vis. spectra of complexes* ***RPIsa 1-4*** *recorded in DMSO with path length 1 cm. (Inset: Expanded spectra of* ***RPIsa-3*** *and* ***4*** *to indicate the MLCT band)*

Table 3.6: *UV-Vis. peak assignments and conductance measurements of* ***RPIsa 1-4***

Compound	*Intra-ligand transitions (nm)*		*MLCT dπ-π* transitions (nm)*	*d-d transitions (nm)*	Λ_m *($\Omega^{-1}cm^2mole^{-1}$)*
	*π-π**	*n-π**			
RPIsa-1	226	265, 345	-	679	42.3
RPIsa-2	229	266, 351	480	677	39.5
RPIsa-3	227	264	413	679	38.0
RPIsa-4	226	265	380	-	40.1

All the four complexes **RPFcA 1-4** have molar conductances (1x 10^{-3}M in DMSO) in the range of 39 - 45 $\Omega^{-1}cm^2mole^{-1}$ (*Table 3.6*) suggesting 1:1 electrolytic behavior.

The ESI-MS positive ion spectra of **RPIsa 1-4** given in *Fig. 3.11* show peaks corresponding to their molecular ions at *m/z* = 762.2 (M^+-ClO_4^-) **RPIsa-1**, 762.1 (M^+-ClO_4^-) **RPIsa-2**, 663.5 (M^+-ClO_4^-) **RPIsa-3** and 681.2 (M^+-ClO_4^-) **RPIsa-4** respectively. The negative ion spectra (*Fig. 3.12*) of all the four complexes show a prominent peak at *m/z* = 98.9 attributed to the perchlorate ion present as the counter anion. The *m/z* values (*Table 3.7*) of the molecular ion peaks for **RPIsa 1-4** are consistent with the proposed structures of the complexes.

Table 3.7: *m/z values of complexes* ***RPIsa 1-4****showing fragmentation.*

Compound	*m/z values*	*Fragments*
RPIsa-1	726.2	$[Ru(phen)_2(Isa\text{-}1)]^+$ (M^+ - ClO_4^-)
	525	$[Ru(phen)_2OCH_2NHNH_2]^+$
	98.9	ClO_4^-
RPIsa-2	726.1	$[Ru(phen)_2(Isa\text{-}2)]^+$ (M^+- ClO_4^-)
	525	$[Ru(phen)_2OCH_2NHNH_2]^+$
	98.9	ClO_4^-
RPIsa-3	663.5	$[Ru(phen)_2(Isa\text{-}3)\text{-}2]^+$ (M^+-2- ClO_4^-)
	525	$[Ru(phen)_2OCH_2NHNH_2]^+$
	98.9	ClO_4^-
RPIsa-4	681.2	$[Ru(phen)_2(Isa\text{-}4)]^+$ (M^+ - ClO_4^-)
	525	$[Ru(phen)_2OCH_2NHNH_2]^+$
	98.9	ClO_4^-

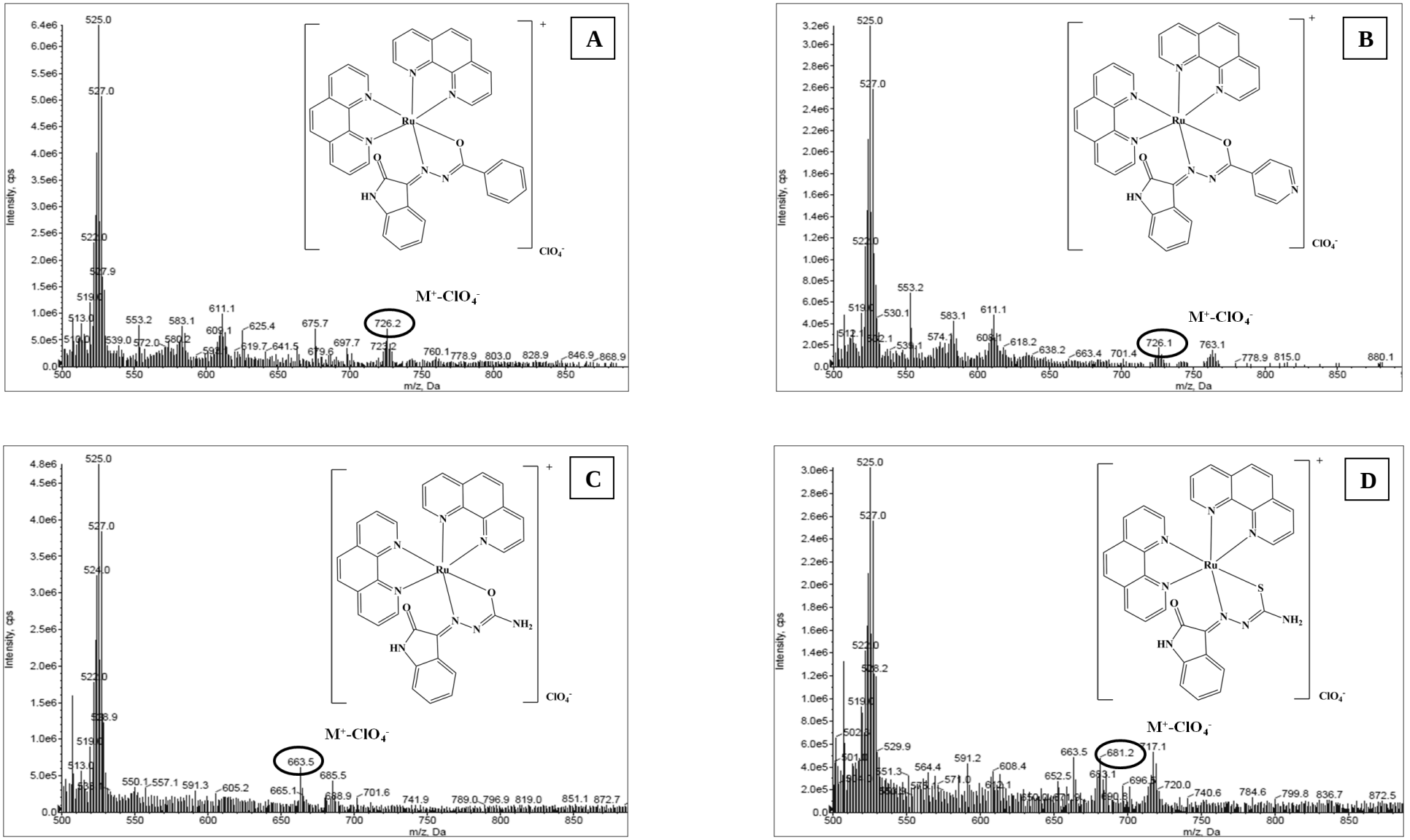

Fig. 3.11: *ESI-MS positive ion spectra of complexes (A)* ***RPIsa-1*** *(B)* ***RPIsa-2*** *(C)* ***RPIsa-3*** *(D)* ***RPIsa-4*** *indicating their molecular ion peak.*

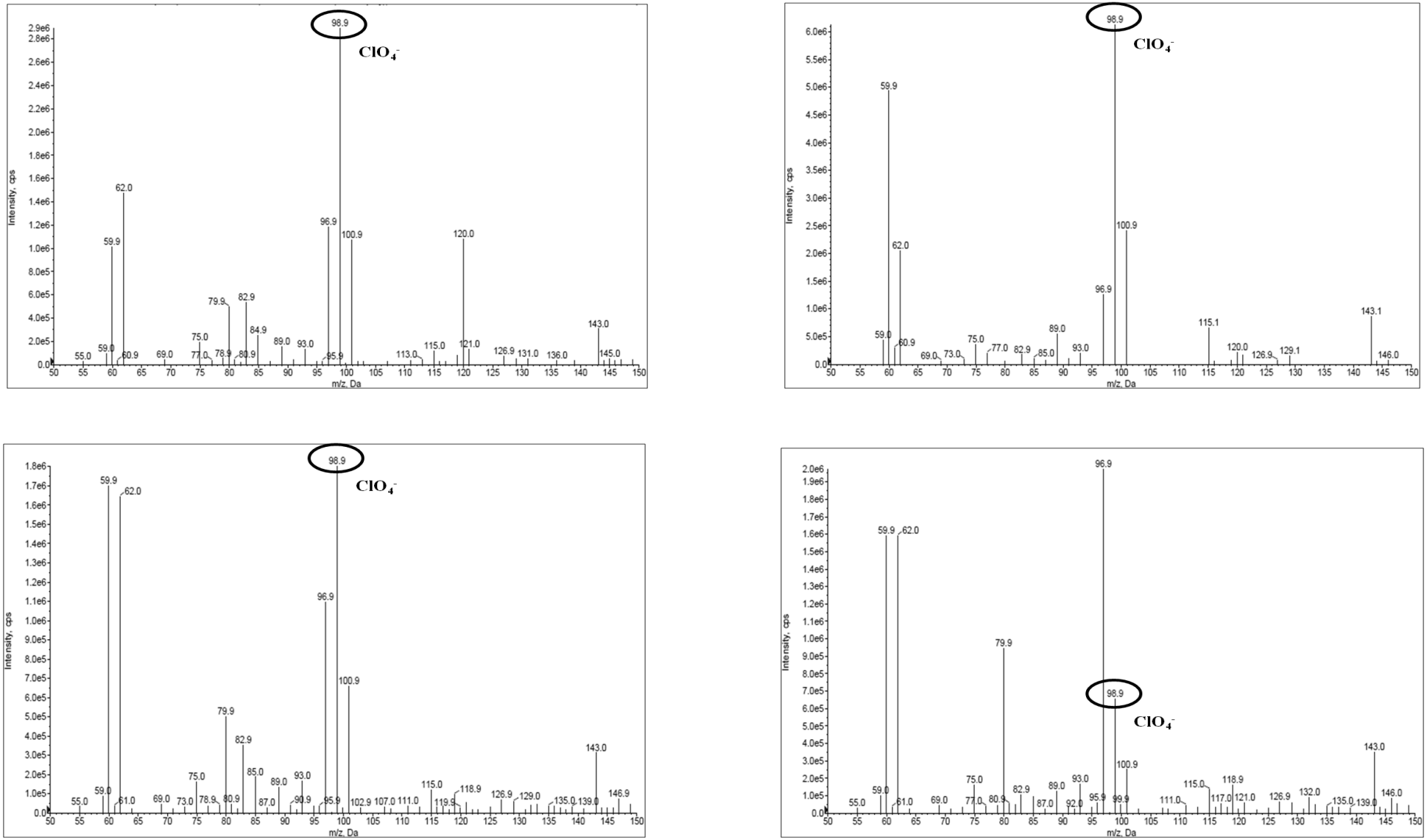

Fig. 3.12: *ESI-MS negative ion spectra of complexes (A)* ***RPIsa-1*** *(B)* ***RPIsa-2*** *(C)* ***RPIsa-3*** *(D)* ***RPIsa-4*** *indicating perchlorate ion peak.*

3.6 [Ru(phen)$_2$ (Flq 1-3)]ClO$_4$ complexes: (RPFlq 1-3)

3.6.1 Synthesis and characterization:

[Ru(phen)$_2$(Flq-1)]ClO$_4$ **(RPFlq-1):**

[Ru(*phen*)$_2$Cl$_2$] 2H$_2$O (0.0528 mmol, 30.0 mg) and **Flq-1** (0.0528 mmol, 18.5 mg) was used to synthesize **RPFlq-1**. Solubility: DMSO, DMF. Yield: 54.29%; Molecular Weight 914.30 g/mol; Molecular Formula $C_{41}H_{37}ClF_2N_7O_7Ru$; Anal. Found: C, 51.98; H, 4.02; N, 9.56. Calc.: C, 53.86; H, 4.08; N, 10.72. ESI-MS *m/z*: 915 (M^++1), 814.3 (M^+-ClO_4^-), 98.9 (ClO_4^-); FTIR (KBr, ν/cm^{-1}): $\nu_{(pyridone)C=O}$ 1721, $\nu_{COOassym}$ 1617, ν_{COOsym} 1329, $\Delta\nu_{COO}$ 288, ν_{Cl-O} 651.

[Ru(phen)$_2$(Flq-2)]ClO$_4$ **(RPFlq-2):**

[Ru(*phen*)$_2$Cl$_2$] 2H$_2$O (0.0528 mmol, 30.0 mg) and **Flq-2** (0.0528 mmol, 19.0 mg) was used to synthesize **RPFlq-2**. Solubility: DMSO, DMF. Yield: 66.78%; Molecular Weight 922.30 g/mol; Molecular Formula $C_{42}H_{36}ClFN_7O_8Ru$; Anal. Found: C, 53.95; H, 3.46; N, 9.23. Calc.: C, 54.69; H, 3.93; N, 10.63. ESI-MS *m/z*: 922.4 (M^+), 822.3 (M^+-ClO_4^-), 98.9 (ClO_4^-); FTIR (KBr, ν/cm^{-1}): $\nu_{(pyridone)C=O}$ 1724, $\nu_{COOassym}$ 1623, ν_{COOsym} 1337, $\Delta\nu_{COO}$ 286, ν_{Cl-O} 650.

[Ru(phen)$_2$(Flq-3)]ClO$_4$ **(RPFlq-3):**

[Ru(*phen*)$_2$Cl$_2$] 2H$_2$O (0.0528 mmol, 30.0 mg) and **Flq-3** (0.0528 mmol, 17.0 mg) was used to synthesize **RPFlq-3**. Solubility: DMSO, DMF. Yield: 62.14%; Molecular Weight 892.27 g/mol; Molecular Formula $C_{41}H_{34}ClFN_7O_7Ru$; Anal. Found: C, 51.79; H, 3.55; N, 9.37. Calc.: C, 55.19; H, 3.84; N, 10.99. ESI-MS *m/z*: 792.3 (M^+-ClO_4^-), 98.9 (ClO_4^-); FTIR (KBr, ν/cm^{-1}): $\nu_{(pyridone)C=O}$ 1717, $\nu_{COOassym}$ 1627, ν_{COOsym} 1340, $\Delta\nu_{COO}$ 287, ν_{Cl-O} 668.

3.6.2 Results and discussion:

In the IR spectra of all the three complexes the stretching band of the free –COOH $\nu(C=O)_{carboxylate}$ at 1680-1700 cm^{-1} and ν(O-H) at 3420-3462 cm^{-1} found in the ligand **Flq 1-3** has disappeared in Ru(II) coordinated fluoroquinolones. Two very strong characteristic bands appear in the range of 1617–1627 and 1330–1340 cm^{-1} assigned as ν(COO) asymmetric and symmetric stretching vibrations, respectively. The separation frequency $\Delta\nu = \nu(COO)_{asym} - \nu(COO)_{sym}$ values fall in the range 286–288 cm^{-1} indicating a monodentate coordination mode of the carboxylato group of the ligand [33,34]. The band which should appear at ~1685 cm^{-1} for aromatic ketones assignable to C=O

stretching of the pyridone ring in the free fluoroquinolones has shifted to 1715-1725 cm^{-1} in the complexes suggesting the binding of fluoroquinolones to the metal centre through the pyridone carbonyl oxygen atom. Also in complexes **RPFlq 1-3** bands at 650-668 cm^{-1} are assignable to ν(Cl-O) stretch of the perchlorate ion. The overall changes in the IR spectra suggest that all the three fluoroquinolones act as monoanionic bidentate ligand and interact with the metal center via the pyridone and carboxylate oxygen.

The electronic absorption spectra of the complexes **RPFlq 1-3** (*Fig. 3.13*) show major bands in the wavelength range 200-900 nm. The bands appearing within 250-300 nm region and those obtained as low intensity shoulders in the region 360-380 nm can be assigned to the intra ligand π→π* and *n*→π* transitions respectively of the aromatic rings of the fluoroquinolone ligand as well as the phenanthroline ligand. The band observed within 480-500 nm is assignable to the metal centred dπ→π* MLCT transition. The complexes also show metal centred d-d bands within the range of 700-705 nm. The absorption peak values have been tabulated in *Table 3.8.*

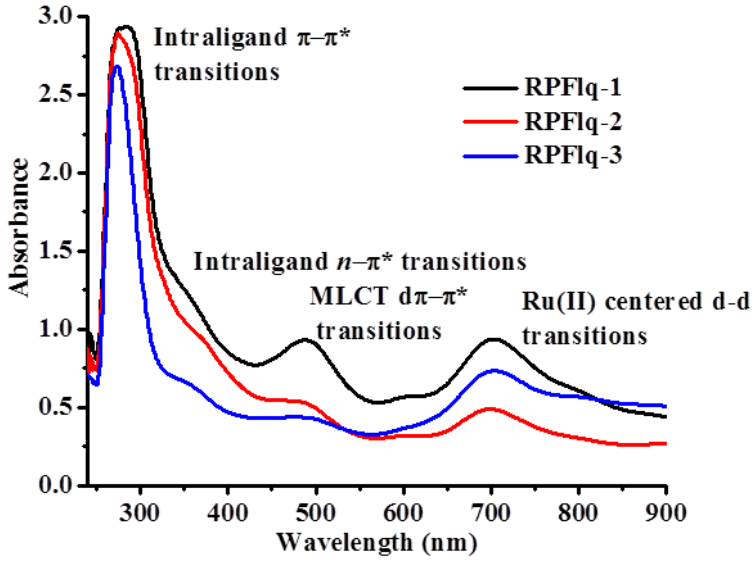

Fig. 3.13: *UV-Vis spectra of complexes* ***RPFlq 1-3*** *recorded in DMSO with path length 1 cm.*

Table 3.8: *UV-Vis. peak assignments and conductance measurements of* ***RPFlq 1-3***

Compound	*Intra-ligand transitions (nm)*		*MLCT dπ-π* transitions (nm)*	*d-d transitions (nm)*	Λ_m $(\Omega^{-1}cm^2mole^{-1})$
	*π-π**	*n-π**			
RPFlq-1	282	360	491	704	25.6
RPFlq-2	279	374	485	704	28.1
RPFlq-3	275	359	493	700	26.4

All the four complexes **RPFcA 1-4** have molar conductances (1x 10^{-3}M in DMSO) in the range of 25 - 28 $\Omega^{-1}cm^2mole^{-1}$ (*Table 3.8*) suggesting 1:1 electrolytic behavior.

The ESI-MS spectra of all the three complexes (*Fig. 3.14*) show *m/z* peaks corresponding to their molecular ion M^+ as well as (M^+-ClO_4^-) in the positive ion spectra and *m/z* peaks corresponding to the perchlorate anion (ClO_4^-) in the negative ion spectra (*Fig. 3.15*). The *m/z* values of the molecular ion peaks for **RPFlq 1-3** (*Table 3.9*) indicate that the two phenanthroline and one fluoroquinolone ligand are coordinated to the Ru(II) metal centre.

Table 3.9: *m/z values of complexes* ***RPFlq 1-3****showing fragmentation.*

Compound	***m/z values***	***Fragments***
RPFlq-1	915	$[Ru(phen)_2(Flq\text{-}1)+1]^+ ClO_4^- (M^++1)$
	814.3	$[Ru(phen)_2(Flq\text{-}1)]^+ (M^+ - ClO_4^-)$
	98.9	ClO_4^-
RPFlq-2	922.4	$[Ru(phen)_2(Flq\text{-}2)]^+ ClO_4^- (M^+)$
	822.3	$[Ru(phen)_2(Flq\text{-}2)]^+ (M^+ - ClO_4^-)$
	98.9	ClO_4^-
RPFlq-3	792.3	$[Ru(phen)_2(Flq\text{-}3)]^+ (M^+ - ClO_4^-)$
	98.9	ClO_4^-

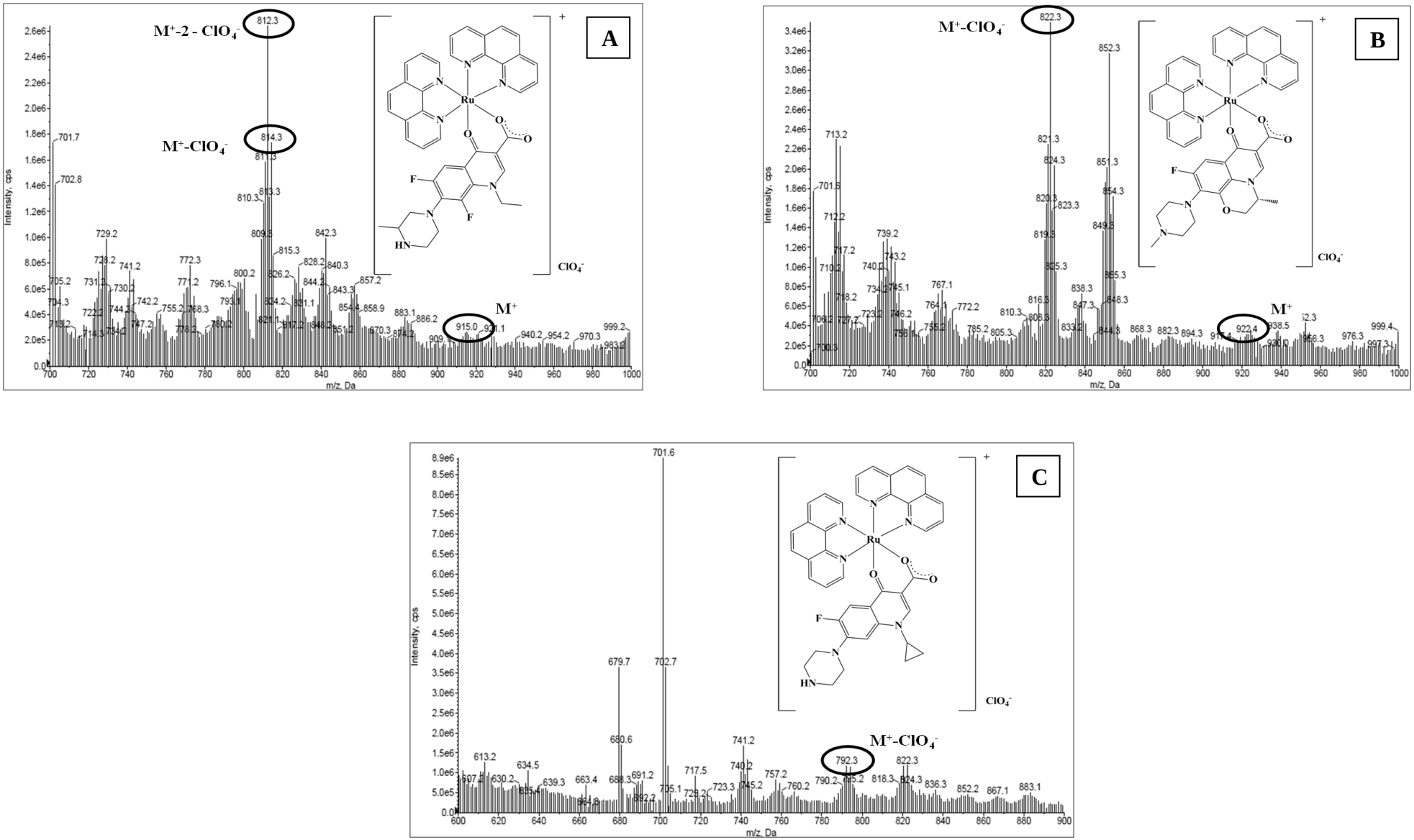

Fig. 3.14: *ESI-MS positive ion spectra of complexes (A)* ***RPFlq-1*** *(B)* ***RPFlq-2*** *(C)* ***RPFlq-3*** *indicating their molecular ion peak.*

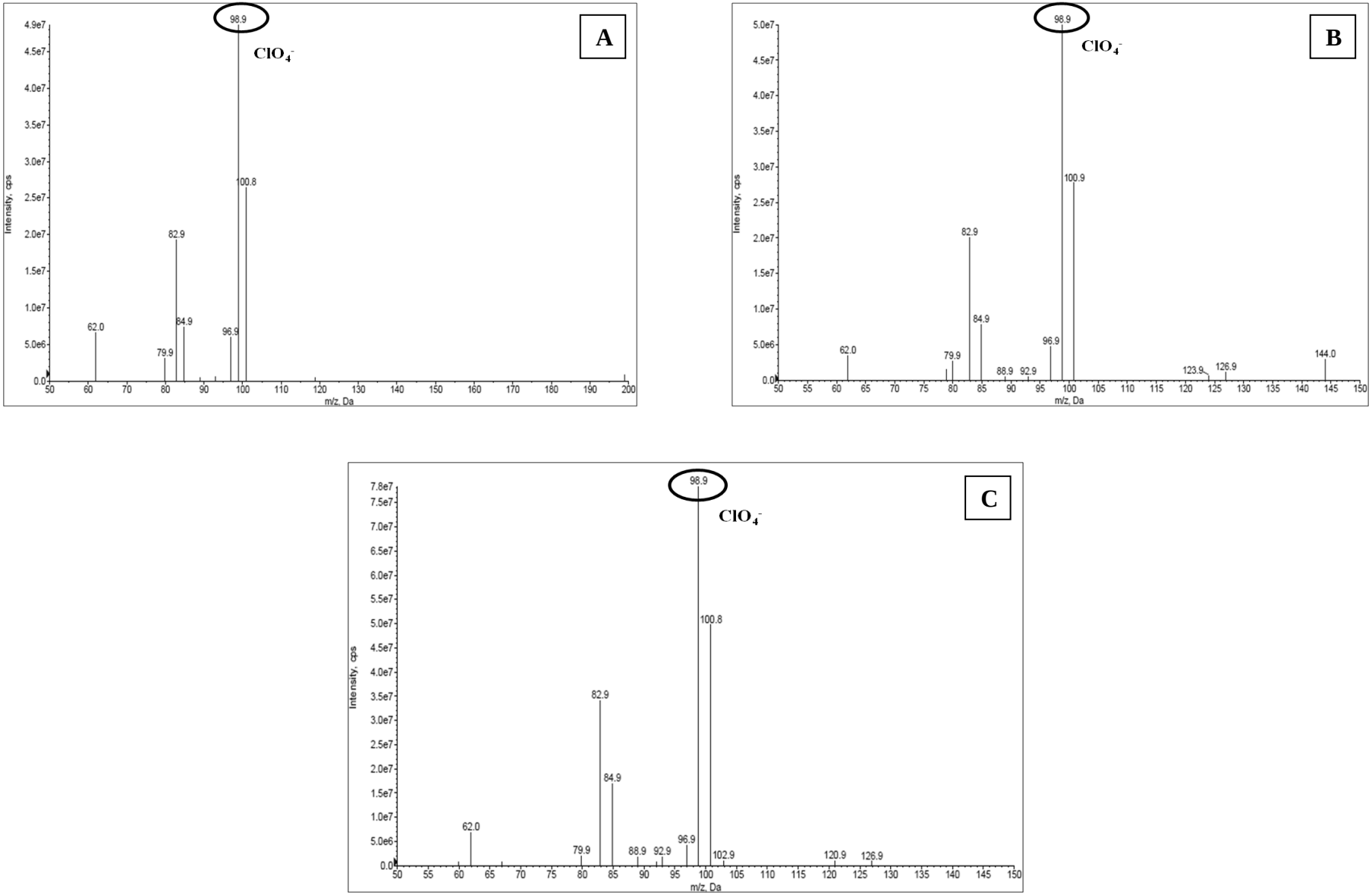

Fig. 3.15: *ESI-MS negative ion spectra of complexes (A)* ***RPFlq-1*** *(B)* ***RPFlq-2*** *(C)* ***RPFlq-3*** *indicating perchlorate ion peak.*

3.7 Summary:

The four different series of $[Ru(phen)_2L]ClO_4$ complex discussed in this chapter have been synthesized and well characterized with an aim to evaluate them for their biomolecular interactions and *in cellulo* anticancer activities.

3.8 References:

[1] Salassa, L. *Eur. J. Inorg. Chem.,* **2011**, 4931.

[2] Zeglis, B. M.; Pierre, V. C.; Barton, J. K. *Chem. Comm.,* **2007**, 4565.

[3] Liu, H. K.; Sadler, P. J. *Acc. Chem. Res.,* **2011**, *44*, 349.

[4] Keene, F. R.; Smith, J. A.; Collins, J. G. *Coord. Chem. Rev.,* **2009**, *253*, 2021.

[5] Nathan, L. K.; Eric, M. *Aust. J. Chem.,* **2012**, *65*, 1325.

[6] Dwyer, F. P.; Gyarfas, E. C.; Rogers, W. P.; Koch, J. H. *Nature,* **1952**, *170*, 190.

[7] Shulman, A.; Dwyer, F. P. *Chelating Agents and Metal Chelates*, Ch. 9, pp. 383–439, **1964**, (Eds F. P. Dwyer, D. P. Mellor) (Academic Press: New York, NY)

[8] Dwyer, F. P. *Aust. J. Sci.,* **1959**, *22*, 240.

[9] Barton, J. K. *Science*, **1986**, *233*, 727.

[10] Schatzschneider, U.; Niesel, J.; Ott, I.; Gust, R.; Alborzinia, H.; Wo¨lfl, S. *Chem. Med. Chem.,* **2008**, *3*, 1104.

[11] Zava, O.; Zakeeruddin, S. M.; Danelon, C.; Vogel, H.; Gra¨tzel, M.; Dyson, P. J. *Chem. Bio. Chem.,* **2009**, *10*, 1796.

[12] Nováková, O.; Kaspárková, J.; Vrána, O.; van Vliet, P. M.; Reedijk, J.; Brabec, V., *Biochemistry,* **1995**, *34*, 12369.

[13] Velders, A. H.; Kooijman, H.; Spek, A. L.; Haasnoot, J. G.; de Vos, D.; Reedijk, J., *Inorg. Chem.,* **2000**, *39*, 2966.

[14] Hotze, A. C. G.; Caspers, S. E.; de Vos, D.; Kooijman, H.; Spek, A. L.; Flamigni,A.; Bacac, M.; Sava, G.; Haasnoot, J. G.; Reedijk, J., *J. Biol. Inorg. Chem.,* **2004**, *9*, 354.

[15] Mishra, L.; Yadaw, A. K.; Sinha, R.; Singh, A. K., *Indian J. Chem. Sect A-Inorg.Bio-Inorg. Phys. Theor. Anal. Chem.,* **2001**, *40*, 913.

[16] Elmes, R. B. P.; Erby, M.; Bright, S. A.; Williams, D. C.; Gunnlaugsson, T. *Chem. Commun.,* **2012**, *48*, 2588.

[17] Concepcion, J. J.; Jurss, J. W.; Brennaman, M. K.; Hoertz, P. G.; Patrocinio, A. O. T.; Iha, N. Y. M.; Templeton, J. L., Meyer, T. J. *Acc. Chem. Res.,* **2009**, *42*, 1954.

[18] Ratanaphan, A; Nhukeaw, T.; Temboot, P.; Hansongnern, K. *Trans. Met. Chem.*, **2012**, *37*, 207.

[19] Xu, L.; Zie, Y.; Zhong, N.; Liang, Z.H.; He, J.; Huang, H.; Liu, Y. *Trans. Met. Chem.*, **2012**, *37*, 197.

[20] Friedman, A. E.; Chambron, J. C.; Sauvage, J. P.; Turro, N. J.; Barton, J. K. *J. Am. Chem. Soc.*, **1990**, *112*, 4960.

[21] Hartshorn, R. M.; Barton, J. K. *J. Am. Chem. Soc*., **1992**, 114, 5919.

[22] Olga, M.; Katarzyna, M.; Barbara, R.; Franck, S.; Claudine, K.; Małgorzata, B. *J. Biol. Inorg. Chem.,* **2014**, *19*, 1305.

[23] Marija, N.; Romana, M.; Ana, B.; Kristina, P.; Ana, R.; Lela, K.; Amela, H.; Marijana, P.; Mario, C. *J. Inorg. Biochem.,* **2016**, *159*, 89.

[24] Sullivan, B. P.; Salmon, D. J.; Meyer, T. J. *Inorg. Chem.,* **1978**, *17*, 334.

[25] Manimaran, A.; Prabhakaran, R.; Deepa, T.; Natarajan, K.; Jayabalakrishnan, C. *Appl. Organometal. Chem.,* **2008**, *22*, 353.

[26] Bottari, B.; Maccari, R.; Monforte, F.; Ottana, R.; Rotondo, E.; Vigorita, M. G. *Bioorg. Med. Chem. Lett.*, **2001**, *11*, 301.

[27] Pejov, L.; Petrusevski, V. M. *J. Phys. Chem. Solids*, **2002**, *63*, 1873.

[28] Çakıra, S.; Biçer, E. *J. Iran Chem. Soc.*, **2010**, *7*, 394.

[29] Khalil, M. M. H.; Aboaly, M. M.; Ramadan, R. M. *Spectrochim. Acta Part A*, **2005**, *61*, 157.

[30] Lu-Ying, L.; Hai-Na. J.; Hui-Jan, Y.; Ke-Jie, D.; Qi-Tian, L.; Kang-Qiang, Q.; Hui, C.; Liang-Nian, J. *J. Inorg. Biochem.*, **2012**, *113*, 31.

[31] Rahmani, F. R.; Sayeed, M.; Malik, A. U.; Ahmad, N. *Proc. Indian Natl. Sci. Acad.*, **1980**, *46A*, 572.

[32] Geary, W. J. *Coord. Chem. Rev.*, **1971**, *7*, 81.

[33] Deacon, G. B.; Phillips, R. J. *Coord. Chem. Rev.*, **1980**, *33*, 227.

[34] Turel, I. *Coord. Chem. Rev.*, **2002**, *232*(1-2), 27.